Progress in understanding W control using ICRH in the JET-ILW tokamak

P.Mantica[1], F.J.Casson[2], M.Valisa[3], C.Angioni[4], R.Bilato[4], E.Belonohy[4], C.Giroud[2], M.Goniche[5], N.Hawkes[2], E. Lerche[6] and JET contributors*

EUROfusion Consortium, JET, Culham Science Centre, Abingdon, OX14 3DB, UK
[1] *Istituto di Fisica del Plasma "P.Caldirola", Consiglio Nazionale delle Ricerche, Milano, Italy*
[2] *CCFE, Culham Science Centre, Abingdon, OX14 3DB, UK*
[3] *Consorzio RFX, Consiglio Nazionale delle Ricerche, Padova, Italy*
[4] *Max Planck Institut fur Plasmaphysik, Garching, Germany*
[5] *CEA-Cadarache, St. Paul Lez Durance, France*
[6] *LPP-ERM-KMS, Belgian State, TEC partner, Brussels, Belgium*
[*] *See the Appendix of F. Romanelli et al., Proceedings of the 25th IAEA Fusion Energy Conference 2014, Saint Petersburg, Russia*

W transport has been studied intensively in JET with ITER-like wall (ILW), since high performance Hybrid scenarios are presently limited in duration by the onset of W accumulation, whilst Baseline H-modes feature reduced pedestal performance possibly linked with the high gas puff rates needed to keep the W influx low.

In high NBI power JET plasmas, neoclassical W transport is enhanced by poloidal asymmetries due to centrifugal effects and was found to be the dominant player in the central region, giving rise to W accumulation as soon as the n_e profile gets peaked [1]. In addition, at the high collisionalities of baseline scenarios, the poloidal asymmetries cause a reduction of the temperature screening, with partial loss of its beneficial effects against n_e peaking [2]. Baseline scenarios can nevertheless reach stationary conditions due to the W expelling effect of sawteeth and less pronounced n_e peaking. Hybrid scenarios, instead, although reaching better performance in the initial phase when n_e is flat, get rapidly (2-3 s) polluted by W accumulation.

Extrapolation of both scenarios [3, 4] to the high current and 33 MW NBI power expected in next campaigns and in D-T experiments indicates that 1) at the high n_e achievable in baseline scenarios the NBI deposition is shifted towards the outer region, thereby decreasing the central n_e peaking and mitigating the W accumulation; 2) in Hybrids at $n_{e0}<1\ 10^{20}\ m^{-3}$ (required for core transport improvement) the NBI deposition is still central and contributes to peaked n_e profiles and high rotation, both enhancing W accumulation. Therefore the use of ICRH in Hybrid scenarios as a control tool for core W transport is mandatory. First analysis of the effects of central ICRH power on W transport [5] indicates various mechanisms with beneficial effects: reduction of n_e peaking, of rotation, and possible peaking of T_i (all counteracting neoclassical inward convection), increased turbulent transport, additional screening from the fast ion temperature gradient, and poloidal asymmetries due to fast ion temperature anisotropy [6], which may lead to outward neoclassical convection. All these mechanisms require a localized central deposition, maximizing the gradients of the fast ions.

In this paper, experimental studies and related modelling of W transport in H-mode Baseline and Hybrid scenarios with/without ICRH at different radial locations is reported. The main diagnostic used for W is the SXR tomography, as described in detail in [1]. Mo Laser Blow-Off and the associated SXR time behaviour was also used to identify separately the diffusion and convection terms and so provide an even more stringent comparison with theory than by steady-state profiles only. The ICRH deposition has been evaluated with TORIC-SSFPQL [7] and simulations with NEO [8] and linear GKW [9] have been made to study the theory predicted effect of ICRH on W and compare with experimental results, as described in [1,2,5].

Figs.1-6 summarize results for two Baseline discharges at 2.8 T/ 2.5 MA, 85308 with 19 MW NBI and 85307 with 14.7 MW NBI and 4.9 MW ICRH (42.5 MHz, ρ_{dep}~+0.03, n_H/n_D~ 5.5%). One can observe in Fig.1 in presence of ICRH the flattening of n_e and reduction of v_{tor}, decreasing the neoclassical inward convection, the peaking of T_e increasing turbulent transport, and the peaked fast ion profile with $T_\perp/T_\parallel$~ 8. We note that with respect to the ICRH modeling of the same discharge in [5], a lower value of n_H/n_D is used, after an experi-

mental reassessment of the available measurements. Experimentally the discharge with ICRH does not exhibit the strong accumulation seen with NBI only (Figs. 2b and 3c) and has a hollow n_W profile. The NEO+GKW calculated W diffusion (D) and convection (V) profiles in Figs.5-6 indeed show a strong inward convection (and consequently peaked n_W - Fig.4) in the NBI only case, whilst ICRH is able to reverse the sign of the central V, leading to hollow n_W profiles. This effect is already present when considering only the effective fast ion temperature $T_{eff}=(T_{\|}+2T_{\perp R0})/3$, but it is much larger when anisotropy is included. The 2D SXR W emission (Fig.3a) shows the hollow pattern with LFS poloidal asymmetry due to centrifugal effects, as in experiment. We note from Fig.4 that in this case the hollow W profile is due to the direct ICRH fast ion effects and not to the ICRH induced plasma profile modifications (case $T_H=T_i$), which attenuate the peaking but are not enough to reach the reversal.

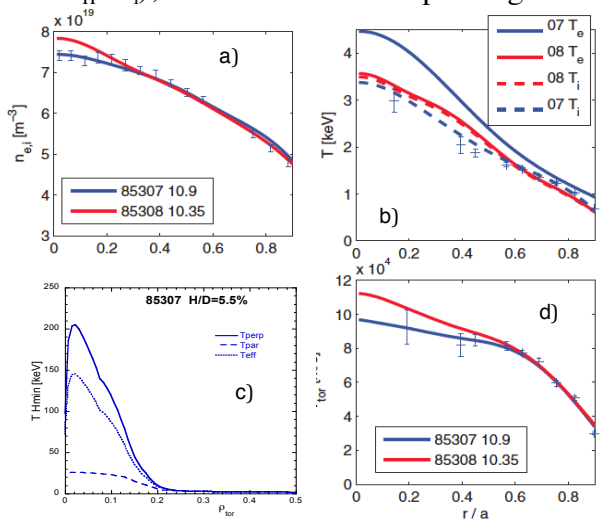

Fig.1: Profile comparison of n_e, T_i, T_e, v_{tor} and ICRH fast ion T_H for baseline shots 85308 (NBI only) and 85307 (NBI+ICRH, H/D=5.5%)

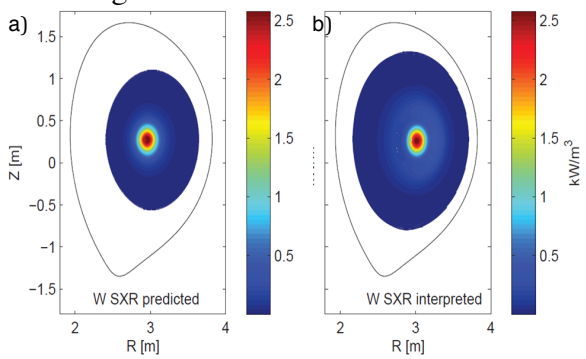

Fig.2: 2D SXR emission due to W in shot 85308 (NBI only) at t=10.35 s: a) NEO+GKW simulation; b) experimental.

Fig.3: 2D SXR emission due to W in shot 85307 (NBI +ICRH, H/D=5.5%), t=10.9s: a) NEO+GKW simulation including fast ion anisotropy; b) NEO+GKW simulation with only fast ion effective temperature; c) experimental.

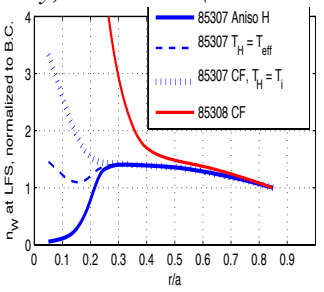

Fig.4: NEO+GKW n_W for 85307–85308. CF = only centrifugal effects

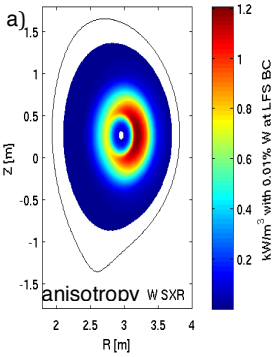

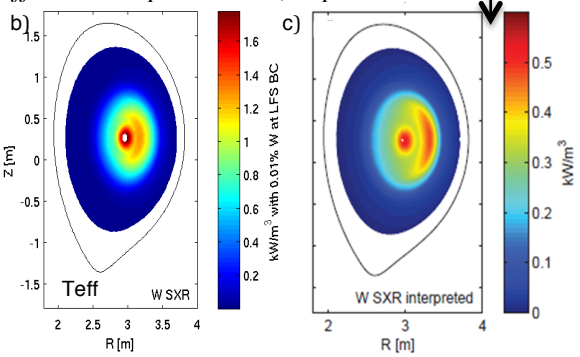

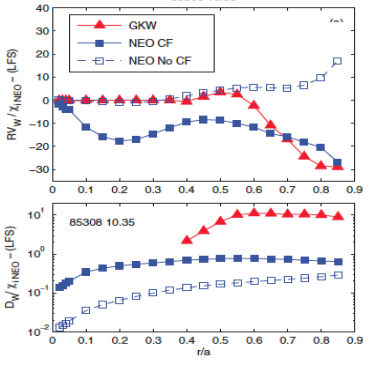

Fig.5: NEO and GKW W D and V profiles for shot 85308

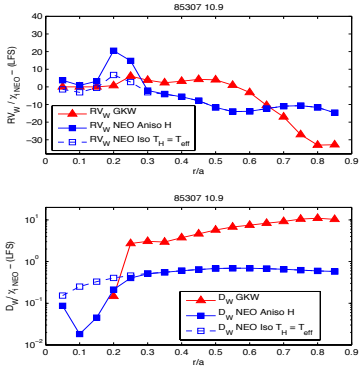

Fig.6: NEO and GKW W D and V profiles for shot 85307

In addition to good agreement between simulated and experimental steady 2D W density profiles, the NEO+ GKW flux surface averaged (FSA) Mo transport coefficients calculated for both shots have been used in time dependent 1D simulations with JETTO-SANCO [10] and UTC SXR post-processor to reproduce the time variation of the SXR line integrals following Mo LBO. As shown in Fig.7, very good

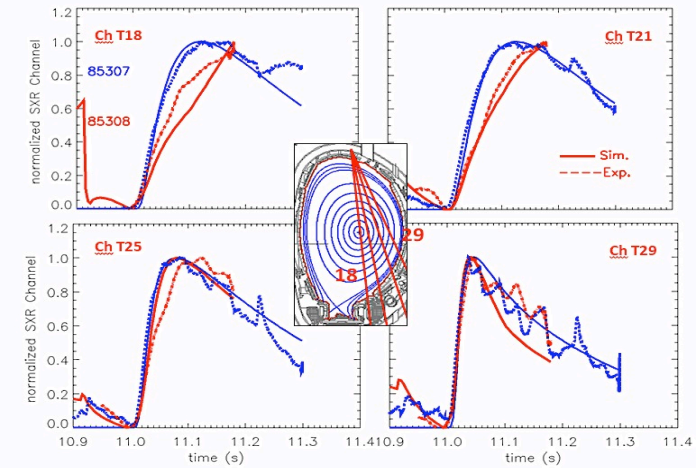

Fig.7: Experimental and NEO+GKW (with anisotropy) time evolution of a few selected channels of the SXR vertical camera during a Mo LBO for discharges 87307 (blue, NBI+ICRH) and 87308 (red, NBI).

agreement is obtained when anisotropy is included. This was not the case for the simulations in [5] at n_H/n_D=9.4%, which shows the sensitivity of the modelling to the ICRH details.

For Hybrid scenarios, we consider two discharges at 2.9 T/2.5 MA, 87253 with 22 MW NBI and 4 MW ICRH (46.2 MHz, ρ_{dep}~-0.14, n_H/n_D~ 4%) and 87252 with 22 MW NBI and 4 MW ICRH (51.4 MHz, ρ_{dep}~-0.4, n_H/n_D~ 4%). It is seen from the experimental SXR tomography (Fig.9) that only the discharge with central ICRH presents hollow W profiles, indicating that W accumulation can be controlled by ICRH in order to extend the scenario duration. Profiles for both shots are shown in Fig.8. In Hybrids due to non-linear e.m. stabilization [11] and low collisionality, T_i can be significantly more peaked than T_e. Unfortunately due to the very low level of C in the central region, the T_i profiles must be obtained from Be CX and are available with large uncertainties and only outside ρ_{tor}~0.3, whilst the central T_i gradient is a key ingredient for this analysis. The choice was to use $T_i = T_e*2.5/(1.5+\rho_{tor})$ which is shown in Fig.8b to lie within the uncertainties of the Be CX profiles where available. It is clear that the large freedom in the T_i profile whose gradient plays a key role in determining neoclassical transport leaves a lot of room in the final W profiles obtained in the simulations. So our purpose here is mainly to investigate which of the various stabilization mechanisms associated to ICRH are at work in these Hybrid shots, and whether within the experimental uncertainties we can reach agreement with the experimental observations.

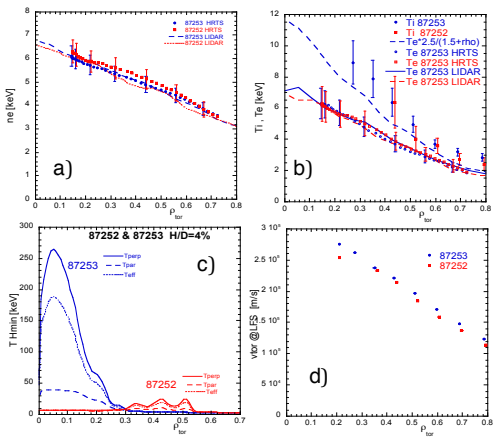

Fig.8: Profiles of n_e, T_i, T_e, v_{tor}, ICRH fast ion temperatures for Hybrid 87253 (blue, ICRH on-axis) and 87252 (red, ICRH off-axis)

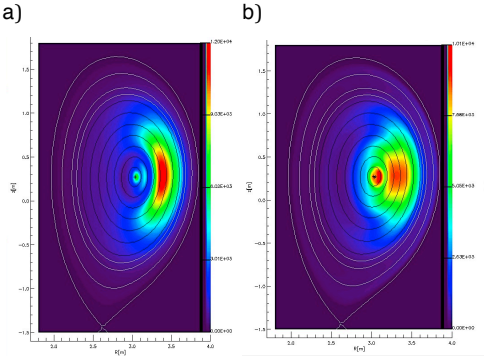

Fig.9: Experimental 2D SXR emission for Hybrid shots a) 87253 (ICRH on-axis) and b) 87252 (ICRH off-axis) at t=6.4s

Fig.8 shows that ICRH has no effect on n_e and T_e, contrary to what seen in the Baseline case, which had a larger ICRH/NBI power ratio. Also the effect on rotation is negligible. The T_i peaking is not expected to change much since ICRH in (H)-D is mainly electron heating. Instead the fast ion T_{eff} and the anisotropy have sharp profiles for the on-axis ICRH case, whilst they are not expected to have any significant effects in the off-axis case (Fig.8c). Therefore we expect that the only mechanism at work to reduce W accumulation in Hybrids is the one associated to direct ICRH effects through fast ion screening and anisotropy. How general this conclusion is will be investigated in future experiments. Fig.10 shows the NEO+GKW calculated W D and V profiles. We note that since the two shots have identical plasma profiles and

off-axis ICRH plays an insignificant role, the curves for 87252 practically coincide with those for 87253 with no ICRH effects included. Fig.11 shows the simulated 2D W SXR emission, which matches well the experimental one, yielding hollow n_W only for the on-axis ICRH shot and only when anisotropy effects are included (Fig.12).

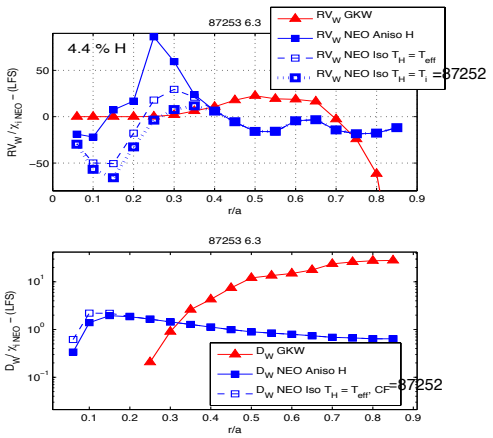

Fig.10: NEO+GKW W D and V profiles for shot 87253 (87252 coincides with 87253 T_H=T_i or CF)

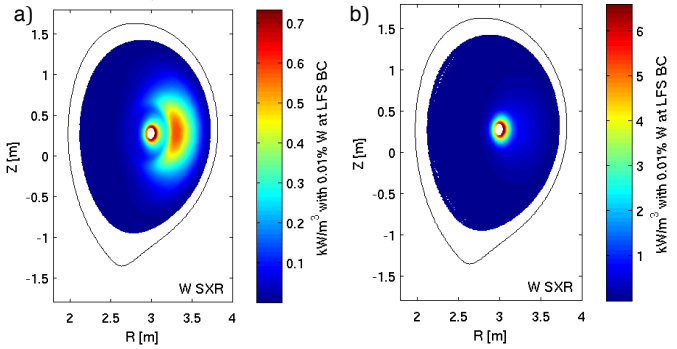

Fig.11: NEO+GKW (with anisotropy) 2D W SXR emission for Hybrid shots a) 87253 and b) 87252

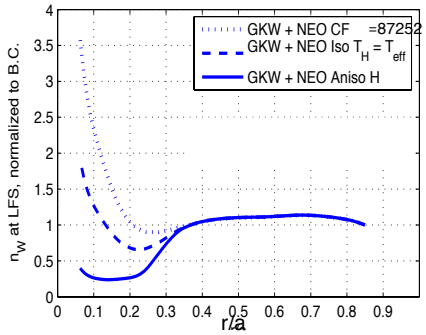

Fig.12: NEO+GKW n_W for 87253 (ICRH on-axis). 87252 (ICRH off-axis) coincides with 87253 CF.

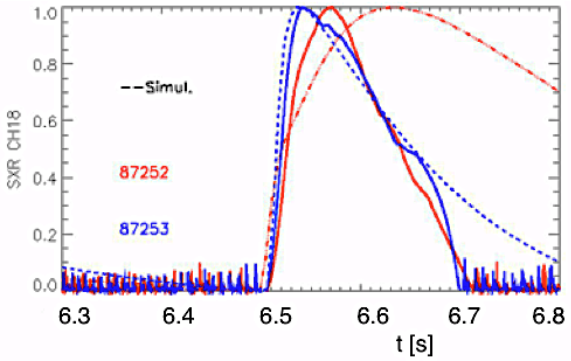

Fig.13: Experimental (full) and simulated (dashed) time evolution of one selected central channel of the SXR vertical camera during a Mo LBO for discharge 87253 (blue, ICRH on-axis) and 87252 (red, ICRH off-axis).

The NEO+GKW FSA Mo transport coefficients have been used in JETTO-SANCO simulations of Mo LBO. In Fig.13 the experimental and simulated SXR time traces indicate good agreement in 87253, whilst accumulation seems overestimated in 87252 (which is visible also in Fig.9b vs Fig.11b), requiring some sensitivity studies within the experimental uncertainties. A scan in minority concentration in simulations (not shown) indicates that when decreasing n_H/n_D the fast ion screening is reduced (as it depends on minority density) and anisotropy effects get comparatively more weight, so overall intermediate n_H/n_D ~4-5% are to be preferred. Concluding, it is found both in experiments and in the modelling that both in Baseline and Hybrid scenarios ICRH with narrow central deposition plays a major role in counteracting W accumulation, with a key role played by fast ion screening and anisotropy, and appears a promising tool to extend the duration of the high performance phase in next JET campaigns.

"This work has been carried out within the framework of the EUROfusion Consortium and has received funding from the Euratom research and training programme 2014-2018 under grant agreement No 633053. The views and opinions expressed herein do not necessarily reflect those of the European Commission."

[1] C.Angioni et al, Nucl. Fusion **54**, 083028 (2014).
[2] C.Angioni et al, Phys. Plasmas **22**, 055902 (2015)
[3] L.Garzotti, private communication
[4] J.Garcia, private communication
[5] F.Casson et al, Plasma Phys. Control. Fusion **57** (2015) 014031
[6] R.Bilato et al., Nucl. Fusion **54**, 072003 (2014)
[7] M. Brambilla and R. Bilato, Nuclear Fusion, **49**, 085004 (2009)
[8] E.Belli and J.Candy, Plasma Phys. Control. Fusion, **50**, 095010 (2008)
[9] A.G. Peeters et al, Comput. Phys. Commun. **180**, 2650 (2009)
[10] Lauro Taroni L. et al, Proc. 21st EPS Conf. on Controlled Fusion and Plasma Physics (Montpellier, France, 1994) vol 1, p 102
[11] J.Citrin et al., PRL **111**, 155001 (2013)